PEG's impact as a plasticizer on the PVA polymer's structural, thermal, mechanical, optical, and dielectric characteristics

M. I. Mohammed[1,2] · **F. El-Sayed**[2]

Abstract

An array of water-soluble polymer blends composed of polyvinyl alcohol (PVA) and poly-ethylene glycol (PEG) have been synthesized by the solution casting technique. The prepared blends were tested using X-ray diffraction (XRD), differential scanning calorimetry, mechanical, optical, and dielectric measurements. According to the XRD studies, PEG has a significant plasticizing impact on PVA, as evidenced by the drop in crystallinity (X_c) values from 31.24 to 25.45%. The thermal study reveals the reduction in the glass transition temperature T_g from 89.2 to 60.6 °C. The outcomes showed that adding PEG affects the mechanical characteristics of PVA/PEG blends, and the ideal blend was one with 25 wt% of PEG loading, where the value of the percentage elongation at break (78%), Toughness (0.44) and surface energy (0.076) reached the highest values at this blend. Meanwhile, Young's modulus declined from 20.34 MPa for pure PVA to 7.07 MPa at 25 wt% PEG. According to the optical studies, the absorption edge shifted from 5.24 to 4.26 eV while the optical band gap (E_g^{ind}, E_g^d) decreased from 4.81, 5.46 eV (pure PVA) to 3.77, 5.04 eV (PVA/PEG30%) respectively, which indicates that forming charge transfer complexes between PVA and PEG polymer. The E_U values enhanced from 0.238 to 1.296 eV and the refractive index improved from 1.38 to 2.97 when PEG content increased. The dielectric and conduction properties were studied from 100 Hz to 1 MHz. It was demonstrated that the dielectric constant ($\varepsilon\prime$) and dielectric loss ($\varepsilon\prime\prime$) are highly frequency-dependent. In addition to that, ($\varepsilon\prime$, $\varepsilon\prime\prime$) values improved from (30, 2) for PVA to (44.46 and 5.39) for PVA/30 wt% PEG blend at 100 Hz, respectively. At the same time, the AC electrical conductivity is improved by increasing the PEG content. These results will likely have far-reaching consequences across a variety of fields, the possible applications due to the increased flexibility of PVA film are flexible packaging, biomedical materials, and other industries that need adaptive and flexible materials. Furthermore, the improved refractive index of the PVA/PEG combination demonstrates its appropriateness for certain applications such as optoelectronic equipment, waveguides, anti-reflective coats, and LEDs. This blend has uses in charge storage devices, such as embedded capacitors due to the enhancement of dielectric constant. Finally, one can say that the research samples have multifunctional applications.

Keywords PVA · PEG · Blend membrane · Flexibility · Mechanical · Optical · Dielectric parameters

---

Extended author information available on the last page of the article

1 Introduction

In the current era of polymer development, polymer blending is crucial to create novel substances with a wide range of desirable qualities. Polymer blends can to adjust the attributes of a finished product to meet the specific needs of the application (Mohammed et al. 2022a, b). The simpler fabrication method and the ability to easily manage the characteristics of polymer electrolytes by varying the blended polymer composition (Mohammed et al. 2023) both suggest that polymeric blends may be preferable.

Polyvinyl alcohol (PVA) is one of the most widely used human-friendly polymers. It's a remarkable synthetic polymer with the added benefits of being non-toxic and biodegradable. PVA is a typical polar polymer with a simple chemical structure and an abundance of attached hydroxyl groups which makes PVA modification possible through simple chemical reactions. PVA has exceptional overall performance, including thermal properties, acceptable biocompatibility, and excellent barrier qualities, making it a potential candidate for some tissue engineering applications, including bone, cartilage, and heart valves (Mohammed et al. 2023; Mohammed et al. 2022a, b). Due to its poor mechanical properties, PVA can be blended with plasticizers to improve its flexibility, and stretchability by modifying the mechanical properties making the films more ductile, and lowering the T_g of the product without altering the fundamental chemical character of the plasticized material (Caicedo et al. 2022; Muhammed et al. 2015). Plasticizer blended with polymer increases the free volume between the polymer chains which allows the chain segments to move and rotate more freely allowing for increased movement of polymer chains to each other, consequently, decreasing the polymer T_g. and tensile strength (TS) while increasing elongation at break (%). Chemicals like sorbitol, citric acid, urea, polyethylene glycol, glycerol and others are commonly employed as plasticizers (Falqi et al. 2018). One of the most often used plasticizers, polyethylene glycol (PEG) is made up of $(CH_2–CH_2–O)n$ linear polymer chains with two hydroxyl groups on each end. Because of its simple structure, it has a high enthalpy and can easily crystallize. PEG is a polymer with the flexible backbone that is water-soluble biodegradable, biocompatible, and nontoxic (Decai et al. 2018). Also, its significant physical and chemical properties enable it to be used in various applications in industry.

Hanpin et al. (2013) investigated the impact of several plasticizers on the mechanical characteristics of Solplus. It was found that the values of T_g and mechanical parameters (tensile strength, Young's modulus, percent elongation, and toughness) were all reduced by all four plasticizers. PEG-6 is the most effective plasticizer at altering the mechanical characteristics of the films out of all the ones evaluated. Abdalla et al. (2004) concluded that the PVA/PEG mixture has shown limited compatibility in the range of 0–30% PEG.

This research aims is to overcome the brittleness and enhance of the flexibility of the PVA membrane by using different concentrations of PEG and determining the ideal concentration of PEG that can increase the flexibility. The improvement of flexibility will be verified by studying the effect of PEG concentration on T_g. The effect of PEG concentrations on the degree of crystallinity of films will be calculated by XRD analysis. The effect of PEG as a plasticizer on the mechanical properties of PVA will be studied and the mechanical parameters will be calculated such as Young's modulus (E), tensile strength (σ), toughness, ductility, and surface energy (γ). Analysis of the optical properties such as energy bandgap, refractive index, and extinction coefficient of the as-prepared films will be carried out in great detail. Impedance spectroscopy can be used to measure the electrical and dielectric properties of materials over a variety of frequencies.
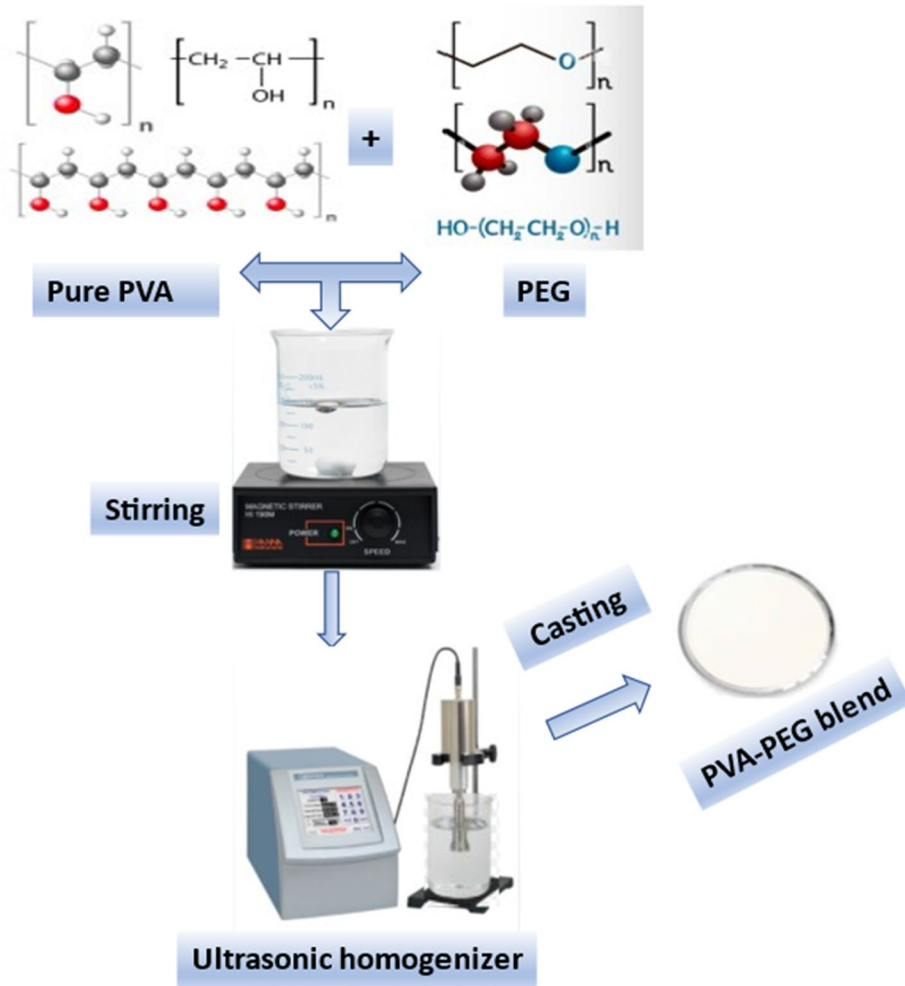
Scheme 1 Schematic diagram of the synthesis of PVA-PEG blend

2 Experimental

2.1 Materials and film preparation

Polyethylene glycol (PEG) (powder, molecular *weight* = 4000 g/mol) and polyvinyl alcohol (PVA) (degree of *hydrolysis* = 99%, molecular *weight* = 27,000 g/mol) were provided by Sigma-Aldrich Company, USA. The solution cast method was used to prepare the films of pure PVA and PEG/PVA blends with PEG loadings of 5, 10, 15, 20, 25, and 30 wt% were found to produce acceptable films with good transparency after numerous experiments. The blends were able to obtain films with satisfactory transparency (as determined by visual observation). Scheme 1 represents a Schematic diagram of the synthesis of the PVA-PEG blend. Characterization and investigation of the resulting films were carried out.

2.2 Characterization techniques and devices

The structure of produced films can be evaluated using the X-ray diffraction technique (XRD-6000 Shimadzu) with CuK_α radiation (1.5405Å) in a 2θ range 10–70°. Differential scanning calorimeters were used to evaluate the glass transition temperature (T_g), and composite melting behavior (T_m) at a heat rate of 10 °C/min under N_2 from 50 to 220 °C (Shimadzu DSC-50).

The mechanical behavior of pure PVA and PVA/PEG blends was determined by using a tensile testing machine (AMETEK, USA). The strain measurement precision was approximately 0.1 mm. Throughout the experiment, the elongation rate was kept constant at 6 mm/min. an optical spectrophotometer is a sophisticated tool for examining how PEG concentration affects the microstructure of polymers by measuring optical properties like absorbance, transmittance, and reflectance with wavelengths at room temperature and normal incidence. The composites' AC electrical conductivity and dielectric characteristics were measured by a programmable automatic LCR meter (Model FLUKE-PM6306). Using a 100 Hz to 1 MHz frequency range, the impedance Z, capacitance C, and loss-tangent ($tan\delta$) were all measured at room temperature.

3 Results and discussion

3.1 X-ray diffraction of PVA /PEG blends

To further understand PEG's effect on the crystal structure of PVA, X-ray diffraction was used, as illustrated in Fig. 1. Because of the strong interaction between hydrogen bonding at the chain polymer, pure PVA revealed a semicrystalline structure and diffraction peak of the plane (101) at around $2\theta = 19.33°$ (major crystalline peak) (Chen et al. 2018). This diffraction peak's intensity decreases as the PEG content increases. The lack of a noticeable
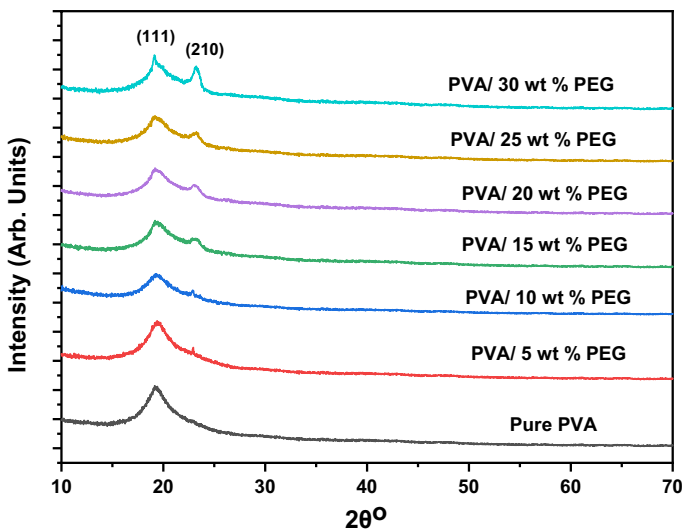

Fig. 1 XRD pattern of pure PVA and PVA / PEG blend films

diffraction peak in the films suggests that the amorphous phase is predominant, which could boost ion conductivity (Nangia et al. 2018).

The first-order reflection was used to calculate the interatomic spacing (d-spacing) values using Bragg's equation ($n\lambda = 2d\sin\theta$) for the films (Nangia et al. 2018). Table 1 reveals that the incorporation of PEG in the PVA matrix does not significantly impact the change in the d-spacing between the pure PVA and PVA/PEG films.

The variation of the degree of crystallinity (X_c) values with different concentrations of PEG was calculated by Eq. 1 (tabulated in Table 1) (Yahia et al. 2019).

$$X_C = \frac{A_{\text{crystalline}}}{A_{\text{crystalline}} + KA_{\text{amorphous}}} \tag{1}$$

$A_{crystalline}$ and $A_{amorphous}$ are the areas of crystalline and amorphous halo reflections, respectively, and K is constant and equal to unity. The calculated values of the degree of crystallinity of the as-prepared films are tabulated in Table 1. One can see from Table 1 the decrease in X_C from 31.24% for PVA to 25.45% for PVA/PEG (30%). The results indicate that PVA films' structure becomes more complicated as a result of molecular interference leading to increased molecular entanglement or decreasing polymer crystallization (Ali and Essa 2014). He et al. (2009) resulting that the degree of crystallinity of chitosan decreased from 28.96% of pure chitosan to 4.34% of chitosan/PEG (5/5). Panova et al. (2020) indicated that the degree of crystallinity of PVA film decreased from 49% for pure PVA to 42% for PVA/ 10 wt% glycerol.

3.2 Differential scanning calorimetry (DSC) of PVA/PEG blends

For studying polymeric materials' thermal characteristics, DSC is an excellent technique. There are thermograms of polyvinyl alcohol and PVA/PEG blends with varying concentrations of PEG (as shown in Fig. 2). The predicted values of the glass transition temperature (T_g) and melting temperature (T_m) are recorded in Table 2.

Figure 2 shows T_g, endothermic peak, of Pure PVA and PVA/PEG blends in the low-temperature area. One can see from Table 2 the significant decrease in the glass transition temperatures with the addition of PEG: it drops from 89.2 °C for pure PVA film to 60.6 °C for PVA/PEG containing 30 wt% of PEG. The inclusion of PEG into the PVA polymer led to an increase in free volume between the polymer chains thereby a lowering of T_g values, allowing the chain segments to move and rotate more freely relative to one another (Sakellariou et al. 1994; Liu et al. 2019). From the data on the decrease of the PVA glass

Table 1 Tabulation of the d-spacing (d) and crystallite size (D) values for pure PVA and PVA / PEG blend films

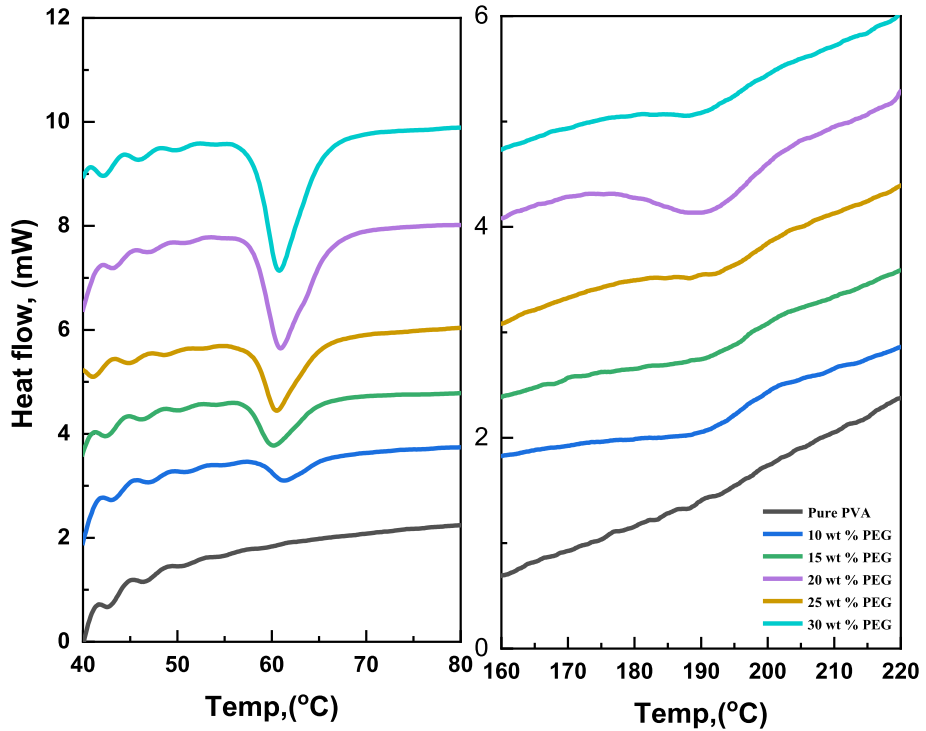| Sample	2θ (°)	FWHM (β, 2θ)	d-Spacing (A°)	XC (%)
Pure PVA	19.26	1	4.607	31.24
PVA/PEG (5%)	19.37	1	4.581	30.87
PVA/PEG (10%)	19.37	1.21	4.581	29.04
PVA/PEG (15%)	19.15	0.95	4.633	26.32
PVA/PEG (20%)	19.17	0.9	4.628	28.05
PVA/PEG (25%)	19.37	0.91	4.581	26.57
PVA/PEG (30%)	19.37	0.45	4.581	25.45

Fig. 2 DSC thermograms of PVA/PEG blend films

Table 2 DSC results of PVA /PEG blend films

The as-produced Polymeric films	Tg, °C	Tm, °C	ΔHm, (J/g)	Refs.
Pure PVA	89.2	188.6	5.25	Present work
PVA/PEG (5 wt%)	63.6	180	4.62	
PVA/PEG (10 wt%)	61.4	179	4.12	
PVA/PEG (15 wt%)	60.3	176	4.12	
PVA/PEG (20 wt%)	60.8	190	6.35	
PVA/PEG (25 wt%)	60.6	188.3	2.59	
PVA/PEG (30 wt%)	60.8	187.8	3.79	
PVA	83	211.78	51.35	Fahad et al. (2018)
PVA/PEG blends	53.85–54.47	214.43–214.21	55.21–42.23	
PVA	82	215	–	Ping et al. (2019)
PVA/PEG blends	52–23	199–171		
PVA	69	224	–	Prajapati et al. (2010)
PVA/H3PO4/PEG (10–40%)	64–68	220–222		

transition temperature with the increase of PEG content, one can conclude that this plasticizer is very effective for PVA (Aharoni 1998). These data are in good agreement with the previous studies. Falqi et al. (2018) showed that T_g decreased from 83 °C of pure PVA

to 51.34 °C by adding 15 wt% of PEG into PVA. Liu et al. (2019) detected that the T_g of pure PVA is 82 °C and T_g s for WPVA/PEG composites are significantly lower and show a continuous descent with the rising of PEG content. Puyou et al. (2016) showed that (T_g) for PVA declined by adding $AlCl_3 \cdot 6H_2O$/glycerin and $AlCl_3 \cdot 6H_2O$/polyglycerin. Prajapati et al. (2010) noticed that T_g decreased from 69 °C of pure PVA to 56 °C for PVA-H_3PO_4-30%PEG (see Table 2).

The second endothermic peaks observed were the melting temperatures T_m for pure PVA and PVA/PEG blends shown in Fig. 2. Table 2 shows that the values of T_m of all blends were not significantly different from those of pure PVA, and its values are equal to 188.6, 180, 179, 176, 190, 188.3 and 187.8 °C for 0, 5, 10, 15, 20, 25 and 30 wt% of PEG content, correspondingly. From the results, one can conclude that PEG did not effect on the T_m of PVA. A similar finding was reported for PVA/PEG blends (Falqi et al. 2018).

3.3 Stress–strain behavior of PVA /PEG blends

Mechanical properties play a major role in both the quality and application of blends. Figure 3 illustrates the stress–strain curves of pure PVA and PVA/PEG blend at room temperature under the strain rate of 3.3×10^{-3} s^{-1}. The mechanical characteristics of PVA and PVA/PEG blend are calculated and tabulated in Table 3. It was noticed from Table 3 that the values of Young's modulus of PVA/PEG blend are less than the value of pure PVA. This result is due to the presence of PEG which increase the chain mobility, thereby, the plasticized polymer would deform at a lower force than without the plasticizer (Hanpin et al. 2013). Also, compared to pure PVA, the inclusion of PEG decreased the tensile strength (as seen in Table 3). This decrease can be due to the plasticizing impact of PEG on pure PVA matrix (Durmaz and Aytac 2021). This result is agreed with other reported findings (Falqi et al. 2018; Lim and Stephen 2013; Ali and Essa 2014).
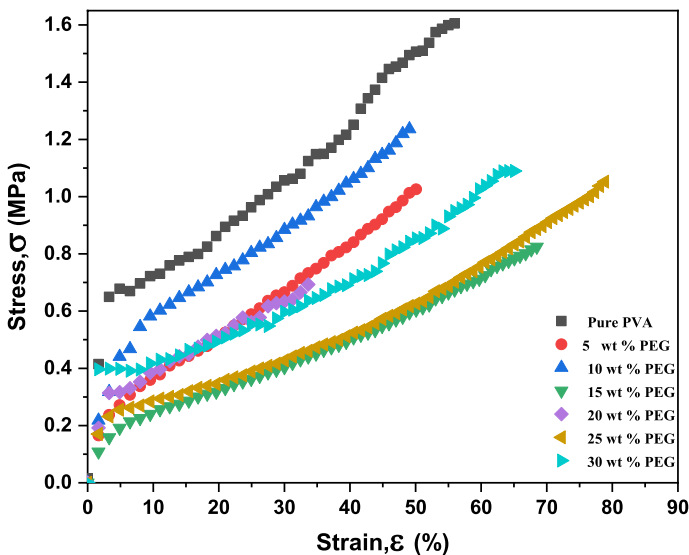

Fig. 3 Stress–Strain curve of pure PVA and PVA/PEG blends

Table 3 Mechanical characteristics of PVA/PEG blend films

The as-produced Polymeric films	Young's modulus E, (MPa)	Tensile strength (σ)	Elongation at break, (ε%)	Toughness	Surface energy (γ)
Pure PVA	20.34	1.58	56	0.58	0.047
PVA/PEG (5 wt%)	10	1.01	50.1	0.39	0.051
PVA/PEG (10 wt%)	13.2	1.22	49.1	0.38	0.056
PVA/PEG (15 wt%)	6.54	0.81	68.5	0.31	0.05
PVA/PEG (20 wt%)	9.57	0.66	33.6	0.15	0.022
PVA/PEG (25 wt%)	7.07	1.04	78.8	0.44	0.076
PVA/PEG (30 wt%)	23.99	1.09	65.1	0.42	0.024

On the contrary, PEG increased the film's elongation at break by up to 25 weight percent due to its ability to increase free volume between polymer chains and hence boost chain mobility and make the films more ductile and flexible (Lim and Stephen 2013). These findings were supported by DSC, which found that increasing the PEG concentration decreased the T_g values of PVA films, enhancing the flexibility of PVA chains. Consequently, Young's modulus dropped and the percentage of elongation at the break rose. Mudigoudra et al. (2012) showed that the content of PEG changed pure PVC from hard and brittle to soft and tough within PVC/PVAc/PEG blended films. Yong et al. (2015) concluded that the T_g of PVA reduced and the flexibility of the PVA chains increased as a result of the addition of $Al(NO_3)_3 \cdot 9H_2O$ (Pu-you et al. 2014). It was observed that adding glycerol to the PVA film caused the T_g to move towards a lower temperature. As a result, the elongation at break increased from 210.58 to 360.20%.

Opposite scenario was seen for the blend containing 30% PEG, the film produced was hard, brittle, and displayed phase separation because of the high PEG content. This caused a substantial fall in its mechanical characteristics, where Young's modulus rose and elongation at break fell (Lim and Stephen 2013).

The total area under the stress–strain curve, which measures the amount of energy a sample can withstand before failing, is a measure of the film's toughness (Davis 2004). The film's strength and ductility are both factors that affect how tough it is Lim and Stephen (2013). From Table 3, it was noticed that film containing 25 wt% of PEG shows the highest toughness, where this film has higher strength and ductility. Puyou et al. (2016) observed that, with the addition of the complex plasticizer ($AlCl_3 \cdot 6H_2O$/glycerin and $AlCl_3 \cdot 6H_2O$/polyglycerin), the plasticized PVA films appeared to be tougher than pure PVA films.

Another helpful parameter for predicting the crack resistance of a film is the tensile strength to Young's modulus ratio (Okhamafe and York 1985). The resistance of a film to the initiation of the fracture process is a measure of the surface energy (γ) and is calculated by Lim and Stephen (2013):

$$\gamma = \left(\frac{\sigma^2 \pi C}{2E} \right) \tag{2}$$

where σ is the tensile strength, C is the flaw or crack size before the initiation of the failure process, and E is Young's modulus. Since the crack size is difficult to measure, the ratio of tensile strength to Young's modulus $\left(\frac{\sigma^2}{2E} \right)$ provides an estimate of crack resistance if C and π are ignored (Okhamafe and York 1985; Jackson 1967). From Table 3, it was noticed that

film containing 25 wt% of PEG shows the highest ratio of tensile strength to Young's modulus, exhibiting the greatest resistance to cracking (0.076). Lim and Stephen (2013) observed that films with 20% w/w PEG-6 have the highest tensile strength to Young's modulus ratio and the highest crack resistance.

3.4 UV–visible studies of pure PVA and PVA/PEG blends

The samples were subjected to ultraviolet -visible (UV–Vis) absorption tests to identify band structure alterations and calculate the optical band gap (Mohammed et al. 2022a,
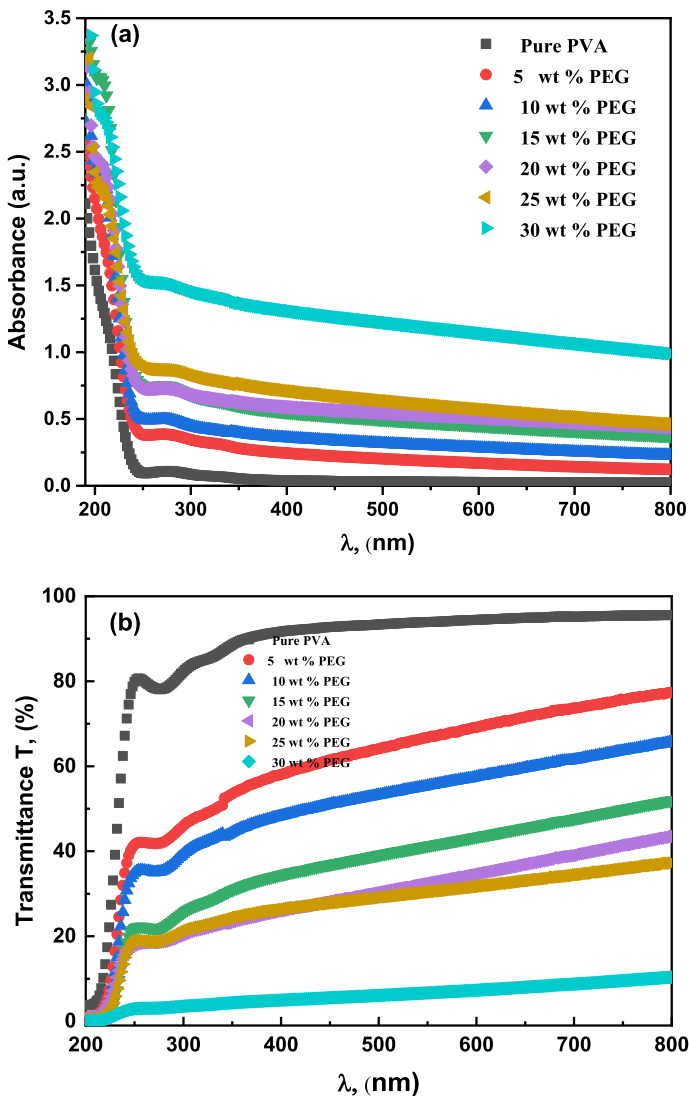
Fig. 4 UV–Vis spectra **a** absorption, and **b** transmission of PVA/PEG blend films

b). In Fig. 4a, the absorption spectra of pure PVA and PVA/PEG blends with various PEG concentrations are displayed. It is possible to attribute the absorption band at 287 nm to the type of electronic transition $\pi \rightarrow \pi^*$, which results from unsaturated bonds, primarily C=O and C=C, that are present in the polymer's tail head (El-Sayed et al. 2020). According to the current findings, there are no absorption peaks at longer wavelengths > 290 nm (Shujahadeen et al. 2020). With a rise in PEG polymer content, all blended samples' absorbance increases. This result showed that the PEG and PVA form an inter/intramolecular hydrogen bond (El-Sayed et al. 2020). Figure 4b shows UV–visible transmission spectra of PVA and PVA/PEG blends with various amounts of PEG in the wavelength range (200–800) nm. Figure 4b indicates that PVA is a transparent polymer with a transmission of 84% in the visible region, and its values rise with wavelength. Also, it is evident from Fig. 4b that the transmission of these films decreased by increasing PEG. This decrease can be assigned to the increase of the disorder within the polymeric samples (Ahmed et al. 2020).

PVA's electronic band structure and the effect of PEG addition are studied in detail to obtain information on the film's light penetration. The optical absorption coefficient was determined using the Lambert–Beer law as follows (Ismail et al. 2021):

$$\alpha = 2.303 * \frac{A}{d} \tag{3}$$

where d is the film thickness, and A is the absorbance. Figure 5a displays the optical absorption coefficient versus incident photon energy of PVA/PEG blends with different concentrations of PEG. The linear extrapolation to zero absorption coefficient ($\alpha = 0$) was used to estimate the location of the absorption edge) E_e (as shown in Fig. 5a and it is noticed that its value shifts from 5.24 eV for the PVA matrix to 4.26 eV for the PVA-30 wt% PEG (see Table 4). This reduction is explained by the development of localized states in the forbidden gap by an increase in PEG content (Ahmed et al. 2020). Also, the absorption coefficient increases as photon energy increases, whereas at lower photon energy, the absorption coefficient α values are constant because the incident photon energy ($h\upsilon$) is insufficient for transferring the electron from the valence band to the conduction band ($h\upsilon < E_g$). While the absorption coefficient value is increased at high photon energy, and therefore, an opportunity for transitions of the electron is more (El-Sayed et al. 2020).

The Urbach energy (E_U) is the amorphous band tail energy, which is fundamental in composites and connected to the absorption coefficient (α) for as-prepared films, by the empirical equation (Urbach 1953):

$$\alpha = \alpha_o e^{\frac{h\upsilon}{E_U}} \tag{4}$$

where α_o, ($h\upsilon$), and (E_U) are constant, photon energy and Urbach's energy, respectively. For pure PVA matrix films and PVA /PEG samples, Fig. 5b shows linear behavior at the fundamental absorption edge in plots of ($\ln(\alpha)$) vs photon energy ($h\upsilon$), showing that these materials obey the empirical Urbach relation (Eq. (4)). It is evident from Table 4 shows that the E_U values enhanced when PEG in blend matrix increased. The increase in the E_U values with increasing the content of PEG in PVA/PEG, as illustrated in Table 4, can be an indication of an increase in the amorphous phase in the blends. However, in the case of PVA, the lesser value of E_U in comparison with those of the blends means that the PVA had a wider energy band gap (Ahmed et al. 2020).

Furthermore, The frequency-dependent absorption coefficient and the optical energy gap E_g obey the classical Tauc's expression (Mott and Davis 1979)
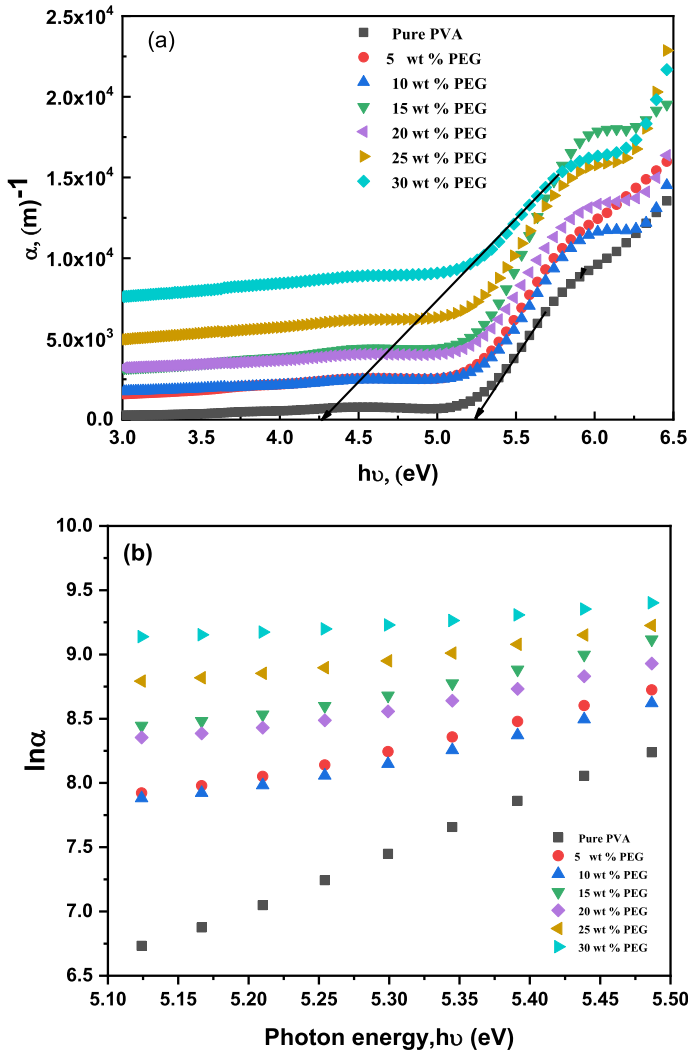
Fig. 5 **a** Absorption coefficient (α) and **b** ln(α) as a function of photon energy ($h\upsilon$) for PVA/PEG blend

$$(\alpha h\upsilon)^{1/2} = B^{1/2}\left(h\upsilon - E_g^{ind}\right) \qquad \text{For indirect allowed transition} \qquad (5)$$

$$(\alpha h\upsilon)^2 = B^2\left(h\upsilon - E_g^d\right) \qquad \text{For direct allowed transition} \qquad (6)$$

where h is Planck's constant, υ is the photon frequency, B is a constant related to the properties of the conduction and valence bands and E_g is the energy gap between the bottom of the conduction band and the top of the valence band at the same value of wave number. The E_g^d and E_g^{ind} were calculated for the prepared blends by plotting photon energy($h\upsilon$) versus $(\alpha h\upsilon)^2$ and $(\alpha h\upsilon)^{1/2}$ as shown in Fig. 6a, b. Table 4 shows that the indirect energy

Table 4 Optical band gap (indirect E_g^{ind} and direct E_g^d), absorption edge E_e, Urbach energy E_U, refractive index (n), absorption index (k) of PVA/PEG blend films

| Polymer blend	E_g^{ind} , (eV)	E_g^d , (eV)	E_e (eV)	E_U (eV)	n	k	Refs.
Pure PVA	4.81	5.46	5.24	0.238	1.38–2.97	0.15–0.29	Present work
PVA/PEG (5%)	4.41	5.32	5.01	0.433			
PVA/PEG (10%)	4.4	5.36	5.046	0.463			
PVA/PEG (15%)	4.39	5.25	4.9	0.508			
PVA/PEG (20%)	4.49	5.26	4.95	0.594			
PVA/PEG (25%)	4.04	5.11	4.4	0.792			
PVA/PEG (30%)	3.77	5.04	4.26	1.296			
PVA	5.26	6.35	6.24	0.22	–	–	Ahmed et al (2020)
PVA/PEG blends	4.91–4.80	6.32–6.34	6.19–6.15	0.24–0.27			
MC-CH-LiBF$_4$/10 wt% PEG	–	4.92–3.78	–	–	–	–	Hawzhin et al. (2019)
PVA	–	–	6.3	0.2	**1.27**	–	Ari et al. (2023)
PVA/PbS NPs	–	–	5.88–5.3	0.62–1.3	**−2.16**	–	
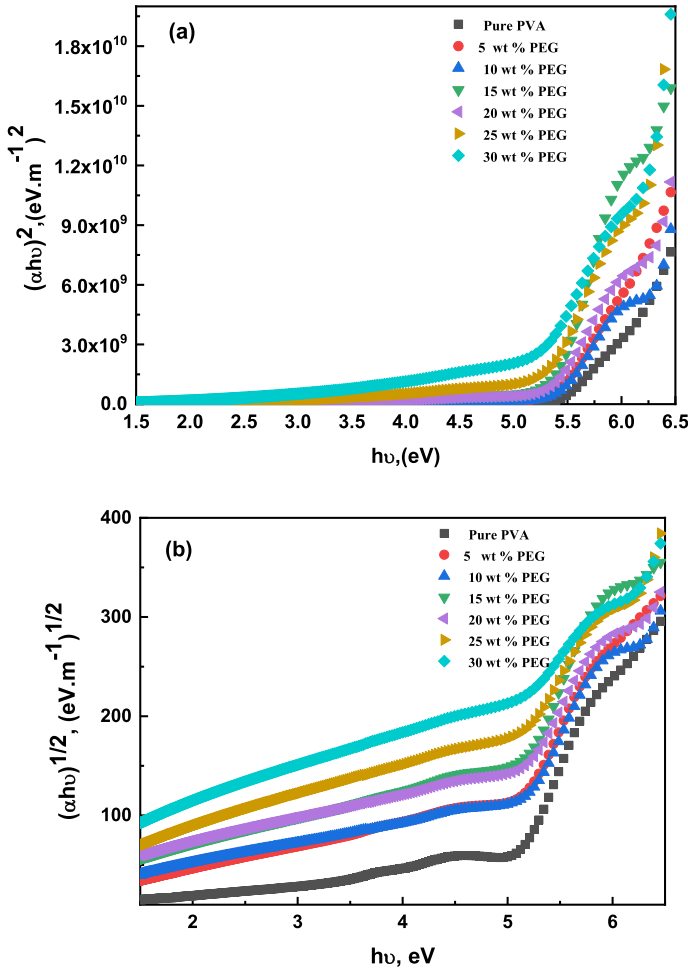
Fig. 6 Tauc plots, **a** direct and **b** indirect band gap for PVA/ PEG blend

gap values decreased from 4.81 to 3.77 eV and the direct energy gap decreased from 5.46 to 5.04 eV as the PEG concentration increases. The decrease in the energy gap values is attributed to the formation of the localized states in the band gap by embedding PEG in PVA (Hawzhin Ahmed et al. 2019). Also, the change in the PVA structure as a result of increasing the disorder degree by adding PEG can explain the decrease in the direct and indirect optical band gap (Hawzhin Ahmed et al. 2019). Hawzhin Ahmed et al. (2019) indicated that the E_g^d values decreased from 4.92 eV for polymer blend electrolyte to 3.78 eV for plasticized with 10 wt% PEG concentration. several reports have also recorded a reduction in PVA's optical bandgap (see Table 4).

The refractive index and extinction coefficient are two optical constants that should always be taken into consideration when selecting materials for an optoelectronic application. There is also a strong connection between an optical material's qualities and its atomic structure, band structure, and electrical properties (Ari et al. 2023). The PVA/ PEG blend's refractive index (n) is shown in Fig. 7a. Using Eq. (7), the refractive index
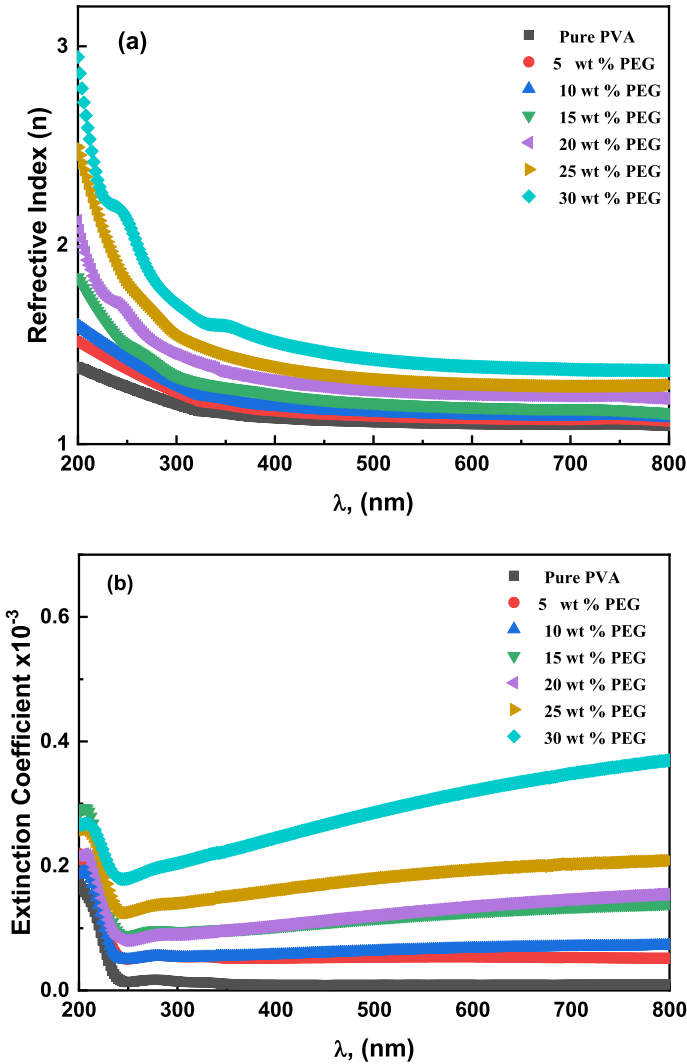
Fig. 7 Variation of **a** refractive index (n), and **b** Extinction coefficient with wavelength for PVA/PEG blend

(n) for the samples was calculated from the reflectance (R) and extinction coefficient (K) (Ahmed et al. 2020):

$$n = \frac{(1+R)}{(1-R)} + \sqrt{\frac{4R}{(R-1)^2} - k^2} \tag{7}$$

Figure 7a shows that increasing the PEG polymer enhanced the refractive index from 1.38 to 2.97 at a low wavelength (200 nm). Add to that it is noticed at low wavelengths, the refractive index exhibits a dispersion zone, while at high wavelengths, the refractive

index is nearly plateau. As a material receives incoming electromagnetic light, the electric field component of the wave causes time-varying forces to act on the material's internal charge structure. Because of the samples' polarity, they had a large dispersion region. At high-wavelength polar molecules, due to their inertia, cannot follow the field alternation (Mohammed et al. 2021). Refractive indices of optical materials must be evaluated for use in integrated optical systems since they are critical design parameters (Yakuphanoglu et al. 2005). The improved refractive index of the PVA/PEG combination demonstrates its appropriateness for certain applications such as optoelectronic equipment, waveguides, anti-reflective coats, and LEDs.

The extinction index (k) was calculated for each sample of the complex refractive index by applying the following formula (El-Sayed et al. 2020),

$$k = \frac{\alpha \lambda}{4\pi} \tag{8}$$

where α is the absorption coefficient of the samples and λ is the wavelength. Figure 7b depicts the variation in k values with wavelength which indicates that light photons and the medium interact. Both absorption and scattering are factors that contribute to the loss of electromagnetic energy in a given material. Figure 7b shows that the extinction coefficient increases as wavelength increases, which is consistent with our prior findings on the extinction coefficient (Ahmed et al. 2020).

3.5 Dielectric and electrical properties.

The dielectric properties of PVA/PEG blends were tested to see if they were suitable for energy storage applications. The complex permittivity $\varepsilon_r^*(\omega)$ is defined by its real and imaginary parts as follows $\varepsilon_r^*(\omega) = \varepsilon\prime(\omega) - j\varepsilon\prime\prime(\omega)$ where $\varepsilon\prime$ is the dielectric constant and $\varepsilon\prime\prime$ is the dielectric loss. Dielectric constant $\varepsilon\prime$ is determined by using the relation (Mohammed 2021):

$$\varepsilon' = \frac{C(F).d(m)}{\varepsilon_o\left(F.m^{-1}\right).A\left(m^2\right)}, \tag{9}$$

$$\varepsilon'' = \varepsilon' \cdot \tan\delta, \tag{10}$$

where C is the parallel capacitance of the film, $(\varepsilon_o = 8.85 \times 10^{-12}$ F/m) is the permittivity of free space, and d, A are the thickness and area of the sample, respectively. Figure 8a displays the variation in the dielectric constant $\varepsilon\prime$ of PVA/PEG blend films as a function of frequency (100 Hz–1 MHz) at room temperature (30 °C), while Fig. 8b displays the frequency dependence of $\varepsilon'\prime$ values for all the prepared films. The two factors are similar in their behaviors, where they attained the highest values in the low-frequency region, and their values decreased with the regular increase in frequency values. The Maxwell–Wagner-Sillar (MWS) effect in PVA/PEG blend was responsible for a significant increase in $\varepsilon\prime$, $\varepsilon'\prime$ at low frequencies (Yassin 2023) where, electric fields vary slowly, giving dipoles (both permanent and induced) time to align themselves with the electric field's direction, resulting in stronger interfacial polarization.

On the contrary, $\varepsilon\prime, \varepsilon'\prime$ displays frequency-independent behavior at higher frequencies, which implies that the dipoles do not rotate quickly enough to reach equilibrium with the electric field (Al-Muntaser et al. 2023; Abdallah et al. 2023).

Fig. 8 **a** Real, **b** imaginary parts of dielectric permittivity, and **c** loss tangent (tanδ) against frequency for all polymeric blend films
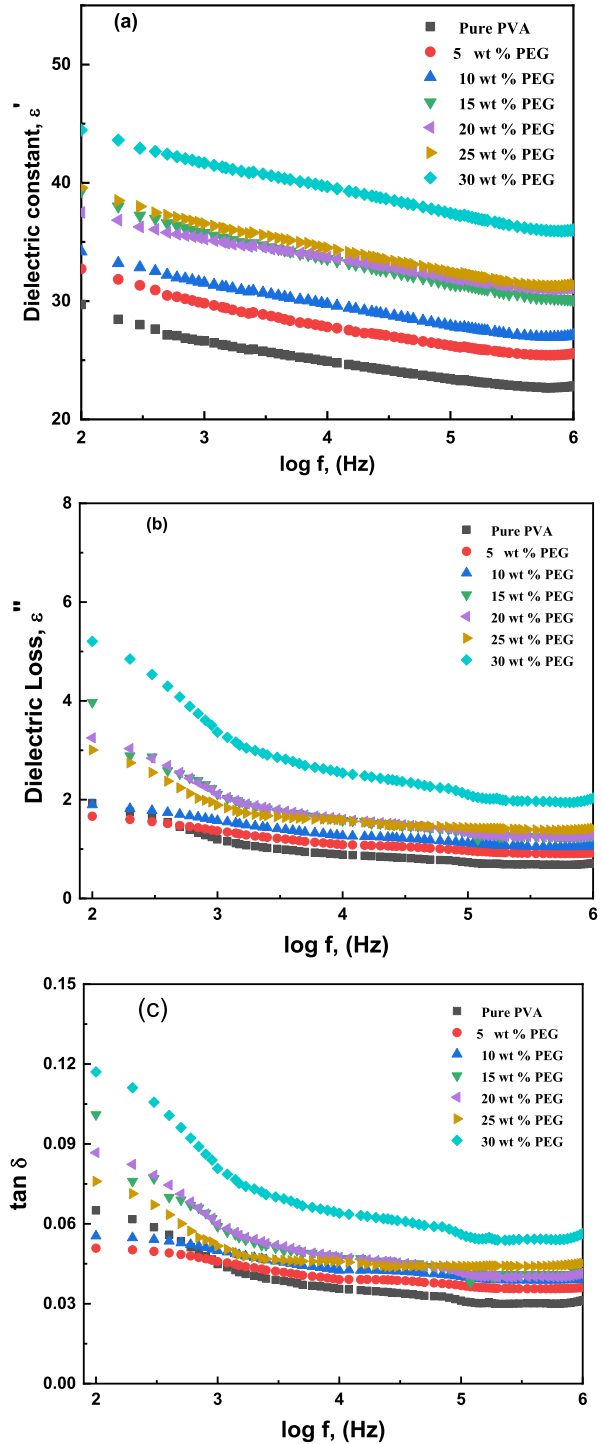
It is important to note that the $\varepsilon\prime, \varepsilon''$ of blends improved as PEG loadings in the blend increased from (30, 2) for PVA to (44.46 and 5.39) for PVA/30 wt% PEG blend at 100 Hz, respectively. The high dielectric constant values of PVA/30 wt% PEG show their ability to store charges when subjected to an electric field. This blend has uses in charge storage devices, such as embedded capacitors.

The change in loss tangent (tan δ) with frequency is shown in Fig. 8c for the as-prepared films. The loss tangent (tan δ) is the ratio of the imaginary part of permittivity to the real part of permittivity or the ratio of energy loss to energy stored. It is evident from Fig. 8c an increase in tan δ in a low-frequency region. Its behavior indicates that the ohmic nature of the samples is more dominant than their capacitive nature. The sudden drop in tan δ values by increasing frequency is due to forming micro-capacitors (Yassin 2023).

The values of the $M^*(\omega)$ spectrum throughout the same frequency range remain close to zero in dielectric materials where the electrode polarization (EP) effect is dominant in the $\varepsilon^*(\omega)$ spectra because the product of these complicated electrode polarization quantities is unity. The reciprocal complex permittivity ε^* is used to compute the dielectric modulus in the following equation (Mohammed 2021; Yassin 2023):

$$M^* = \frac{1}{\varepsilon^*} = \frac{\varepsilon'}{\varepsilon'^2 + \varepsilon''^2} + i\frac{\varepsilon''}{\varepsilon'^2 + \varepsilon''^2}, \tag{11}$$

$$M^* = M' + iM'', \tag{12}$$

The real and imaginary components of the electric modulus are denoted by $M\prime$ and M^ε Accordingly, the complex electric modulus (real part M' and imaginary part M'') spectra of PVA/PEG blend films at 30 °C are presented in Fig. 9a, b. Since the M′ and M″ spectra are free of the electrode polarization (EP) effect, adsorbed impurities, and the electrode material of the dielectric test fixture due to the inverse relationship between the dielectric and electric modulus functions, these spectra are frequently examined for a better resolution of the relaxation processes in composite materials (Yassin 2023). In the low-frequency zone, M′ values gradually grow with an increase in frequency; however, in the high-frequency region, they suddenly climb and eventually reach a steady state about 1 MHz, as shown in Fig. 9a. Many additional materials have M′ spectra that exhibit same dispersion behavior (Sugumaran et al. 2015; Karthikeyan et al. 2016).

According to Fig. 9b, the M" spectra of the films show a minimum at around 1 kHz and a nonlinear increase on either side of the minimum with frequency deviation, indicating that these films have relaxation processes below 100 Hz at 30 °C. These relaxation processes are most likely caused by the side chain dynamics and main chain segments in the PVA-PEG blend structures. Previous studies on M" spectra showed that a variety of materials exhibit relaxation peaks in the 100 Hz–1 MHz region when the polymer chains are significantly more flexible and less constrained by their dynamic processes (Shahbazi et al. 2016; Choudhary 2018).

The equation for determining the total conductivity of dielectric materials (Abdallah et al. 2023):

$$\sigma_{Total.AC}(\omega) = \sigma_{DC}(\omega \rightarrow 0) + \sigma_{AC}(\omega), \quad \left(\text{Joncher's power law}\right) \tag{13}$$

where σ_{Dc} is the DC conductivity at zero frequency, the AC conductivity; $\sigma_{AC} = \omega\varepsilon_o\varepsilon''$ (Mohammed 2021), and the angular frequency is $\omega = 2\pi f$. Figure 10 shows the frequency
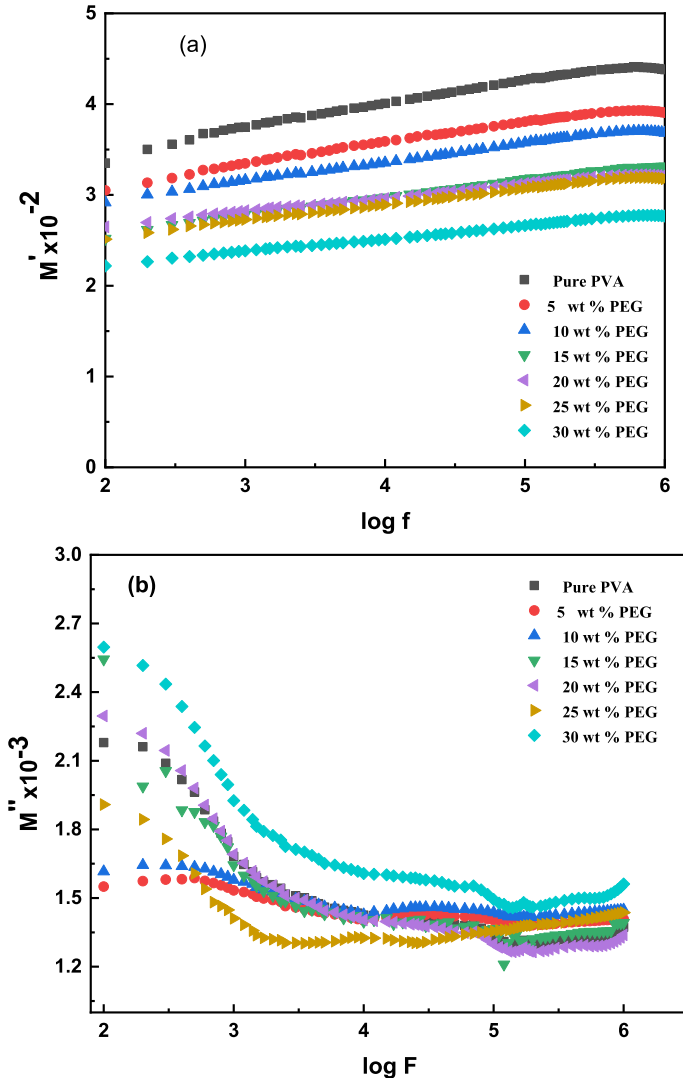
Fig. 9 **a** Real, **b** imaginary parts of electrical modules against frequency for all polymeric blend films

dependence of pure PVA and PVA/PEG blend films' AC electrical conductivity at room temperature.

This trend shows that the hopping mechanism may be playing a key part in the conduction process at low temperatures. It's easy to imagine a link between charge carrier hopping probability and polymeric environment molecular mobility. Localized sites like strong dipoles or charge transfer along the backbone or side groups must be favored by segmental motion (Mohammed 2021).

By extrapolating from the low-frequency zone to $ln\ \sigma_{AC}$, the DC electrical conductivity (σ_{DC}) was attained. The σ_{DC} values at various PEG content are tabulated in Table 5. The σ_{DC} values are found to increase with increasing the PEG content; this indicates the charge hopping conduction mechanism in the examined films.
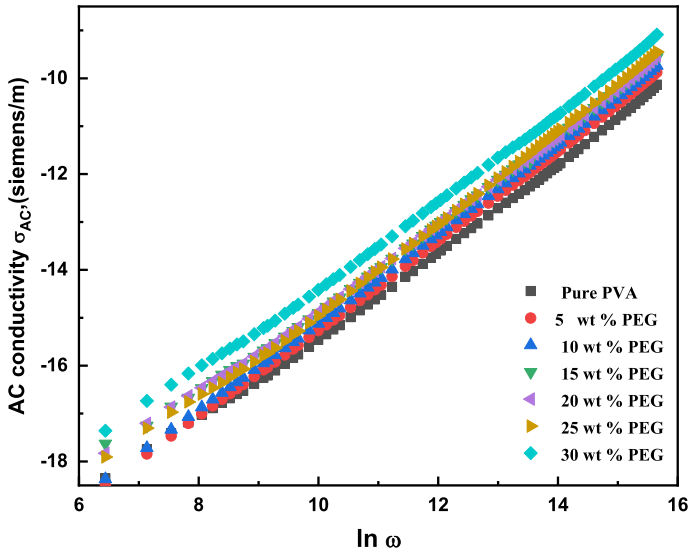
Fig. 10 AC conductivity versus angular frequency for all polymeric blend films

Table 5 σ_{dc} and s parameter of PVA/PEG blend films

$\sigma_{dc} \times 10^{-11}$	s
0.819	0.98055
1.161	0.97591
1.380	0.97407
1.541	0.97803
1.476	0.98126
1.463	0.98884
2.527	0.97539

Most of the time, it has been noticed that the frequency dispersion of σ_{AC} follows the universal power law of ac conductivity: $\sigma_{AC}(\omega) = A\omega^s$, where A is a constant that is independent of temperature, and s is a power-law exponent that ranges from 0 to 1. This power law describes the level of contact between the mobile ions and is connected to the dynamics of hopping transport between states in the forbidden gap. The values of exponent (s) are calculated and tabulated in Table 5. Exponent (s) is found to have a value between 0.980 and 0.975, which is compatible with Elliot's overall characteristics of amorphous nature (El-Sayed et al. 2020; Yahia and Mohammed 2018).

4 Conclusions

PEG was used as a plasticizer to modify the thermal, mechanical, optical, and dielectric properties of PVA film. XRD results showed that the crystallinity of the blend polymer films is decreasing with the amount of PEG increase. By analyzing DSC data, it was found that polyethylene glycol (PEG) significantly reduces the T_g of PVA blends. The mechanical

studies revealed that the addition of PEG enhances the mechanical characteristics of PVA/PEG blends and 25 wt% PEG loading was the optimum blend. With an increase in PEG concentration in the blend, the optical absorption spectra indicated the presence of optical band gaps (direct and indirect) that dropped from 5.46 to 5.04 eV and 4.81 to 3.77 eV, respectively. The dielectric properties study of the prepared blends revealed high dielectric constant and electric modulus by increasing PEG content indicating higher energy storing capability of the material which suggests applications of these films as an interlayer dielectric in organic electronic devices.

Availability of data and materials The data that support the findings of this study are available from the corresponding author upon reasonable request.

Declarations

Competing interest The authors declare that they have no known competing financial interests or personal relationships that could have appeared to influence the work reported in this paper.

Ethical approval This article does not contain any studies with animals performed by any of the authors.

References

Abdallah, S.G., Said, H.M., El-Naggar, M., El-Naggar, A.W.M.: Structural properties of γ-irradiated poly(vinyl alcohol)/poly(ethylene glycol) polymer blends. Appl. Polym. Sci. **94**(1), 167–176 (2004)

Abdallah, E.M., Asnag, G.M., Morsi, M.A., Aljohani, M., Albalwa, A.N., Yassin, A.Y.: Elucidation of the effect of hybrid copper/selenium nanofiller on the optical, thermal, electrical, mechanical properties and antibacterial activity of polyvinyl alcohol/carboxymethyl cellulose blend. Polym. Eng. Sci. **63**(7), 1974–1988 (2023)

Aharoni, S.M.: Increased glass transition temperature in motionally constrained semicrystalline polymers. Polym. Adv. Technol. **9**(3), 169–201 (1998)

Ahmed, H.T., Jalal, V.J., Tahir, D.A., Mohamad, A.H., Abdullah, O.G.: Effect of PEG as a plasticizer on the electrical and optical properties of polymer blend electrolyte MC-CH-LiBF$_4$ based films. Results Phys. **15**, 102735 (2019)

Ahmed, R.M., Ibrahim, A.A., El-Said, E.A.: Enhancing the optical properties of polyvinyl alcohol by blending it with polyethylene glycol. Acta. Phys. Polon. **137**(3), 317–323 (2020)

Ali, Z.I., Essa, W.H.: Characterization of electron beam irradiated poly vinyl alcohol / poly ethylene glycol blends. J. Sci. Res. **6**(1), 29–42 (2014)

Al-Muntaser, A.A., Pashameah, R.A., Saeed, A., Alwafi, R., Alzahrani, E., AlSubhi, S.A., Yassin, A.Y.: Boosting the optical, structural, electrical, and dielectric properties of polystyrene using a hybrid GNP/

Cu nanofiller: novel nanocomposites for energy storage applications. Mater. Sci. Mater. Electron. **34**(7), 678–691(2023)

Caicedo, C., Claudio Cruz, C.A., Regalado, E.J.J., Aguirre-Loredo, R.Y.: Effect of plasticizer content on mechanical and water vapor permeability of maize starch/PVOH/chitosan composite films. Mater. **15**(4), 1274–1285(2022)

Chen, Y.-N., Jiao, C., Zhao, Y., Zhang, J., Wang, H.: Self-assembled polyvinyl alcohol−tannic acid hydrogels with diverse microstructures and good mechanical properties. ACS Omega. **3**(9), 11788–11795 (2018)

Choudhary, S.: Structural, morphological, thermal, dielectric, and electrical Properties of alumina nanoparticles filled PVA–PVP blend matrix-based polymer nanocomposites. Polym. Comp. **39**(S3), 1788–1799 (2018)

Darwesh, A.H., Mohammed, P.A., Mamand, S.M., Hussen, S.A., Aziz, S.B., Brza, M.A., Abdullah, R.M., Karim, W.O.: Investigation of structural and optical characteristics of biopolymer composites based on polyvinyl alcohol inserted with PbS nanoparticles. Coatings. **13**(3), 578–600 (2023)

Davis, J.R.: Tensile testing, 2nd edn. ASM International, Ohio (2004)

Decai, L., Jiang, Y., Lv, S., Liu, X., Gu, J., Chen, Q., Zhang, Y.: Preparation of plasticized poly (lactic acid) and its influence on the properties of composite materials. PLoS One. **13**(3), 1–15 (2018)

Durmaz, B.U., Aytac, A.: Efects of polyol-based plasticizer types and concentration on the properties of polyvinyl alcohol and casein blend films. Polym. Environ. **29**(1), 313–322 (2021)

El-Sayed, F., Mohammed, M.I., Yahia, I.S.: Discussions on the film design and mechanical properties of Y^{3+}/PVA polymeric composite films: enhancement of the electrical conductivity and dielectric properties. Mater. Sci. Mater. Electron. **31**, 10408–10421 (2020)

Fahad, H., Falqi, F.H., Bin-Dahman, O.A., Hussain, M., Al-Harthi, M.A.: Preparation of miscible PVA/PEG blends and effect of graphene concentration on thermal, crystallization, morphological, and mechanical properties of PVA/PEG (10 wt%). Blend Hindawi Int. J. Polym. Sci. 1–10, 8527693 (2018)

Hanpin, L., Hoag, S.W.: Plasticizer effects on physical–mechanical properties of solvent cast soluplus® films. AAPS Pharm. Sci. Tech. **14**(3), 903–910 (2013)

He, L.-H., Xue, R., Yang, D.-B., Liu, Y., Song, R.: Effects of blending chitosan with PEG on surface morphology, crystallization and thermal properties. Polym. Sci. **27**(4), 501–510 (2009)

Ismail, A.M., Mohammed, M.I., Yahia, I.S.: A facile method to prepare g-carbon nitride/poly(vinyl alcohol) nanocomposite films with remarkable optoelectrical properties: laser attenuation approach. Opt. Laser Tech. **134**, 106600 (2021)

Jackson, W.J., Caldwell, J.R.: Antiplasticization. III. Characteristics and properties of antiplasticizable polymers. Appl. Polym. Sci. **11**(2), 227–244 (1967)

Karthikeyan, B., Pandiyarajan, T., Mangalaraja, R.V.: Enhanced blue light emission in transparent ZnO:PVA nanocomposite free standing polymer films. Spectro. Chim. Acta A. **152**, 485–490 (2016)

Liu, P., Chen, W., Liu, C., Tian, M., Liu, P.: A novel poly (vinyl alcohol)/poly (ethylene glycol) scaffold for tissue engineering with a unique bimodal open-celled structure fabricated using supercritical fluid foaming. Sci. Rep.**9**(1), 9534 (2019)

Mohammed, M.I., Bouzidi, A., Zahran, H.Y.: Ammonium iodide salt-doped polyvinyl alcohol polymeric electrolyte for UV-shielding filters: synthesis, optical and dielectric characteristics. Mater. Sci. Mater. Electron. **32**(4), 4416–4436 (2021)

Mohammed, M.I., Yahia, I.S., Abd El-Mongy, S.: Simple fabrication of PVA/PEG blend doped with methyl blue dye with superior optical limiting performance: enhanced luminescence property, structural, and dielectric properties. Mater. Sci. Eng. B **291**, 116390 (2023)

Mohammed, M.I., Yahia, I.S., El-Sayed, F.: Study the microstructure, optical, mechanical, and dielectric characteristics of Cu^{2+}/Zn^{2+}-codoped PVA for CUT-OFF laser filters. Polym. Bull.**80**(60), 8377–8405 (2022a)

Mohammed, M.I., Yahia, I. S., Abd El-Mongy S.: Studying the structural, optical, electrical properties and magnetic properties of Fe^{3+}-codoped Al^{3+}/PVA flexible composite films. Opt. Quant. Electron. **54**(9), 566–588 (2022b)

Mohammed, M.I.: Dielectric dispersion and relaxations in (PMMA/PVDF)/ZnO nanocomposites. Polym. Bull. **79**(7), 2443–2459 (2021)

Mott, N.F., Davis, E.A.: Electronic process in non-crystalline material. Clarendon Press, Oxford (1979)

Mudigoudra, B.S., Masti, S.P., Chougale, R.B.: Investigation of mechanical properties of ternary polymer PVC/PVAc/PEG blended films. Res. Eng. Sci. **1**(2), 63–65 (2012)

Nangia, R., Shukla, N.K., Sharma, A.: Frequency and temperature-dependent impedance spectroscopy of PVA/PEG polymer blend film. High Perform. Polym. **30**(8), 918–926 (2018)

Okhamafe, A.O., York, P.: Stress crack resistance of some pigmented and unpigmented tablet film coating systems. J. Pharm. Pharmacol. **37**(7), 449–454 (1985)

Panova, T.V., Efimova, A.A., Berkovich, A.K., Efimov, A.V.: Plasticity control of poly(vinyl alcohol)–graphene oxide nanocomposites. R. Soc. Chem. **10**, 24027–24036 (2020)

Prajapati, G.K., Roshan, R., Gupta, P.N.: Effect of plasticizer on ionic transport and dielectric properties of PVA–H_3PO_4 proton conducting polymeric electrolytes. Phys. Chem. Solids **71**, 1717–1723 (2010)

Pu-You, J., Cai-ying, B., Li-hong, H., Yong-hong, Z.: Properties of poly (vinyl alcohol) plasticized by glycerine. J. Forest. Prod. Ind. **3**(3), 151–153 (2014)

Puyou, J., Meng, Z., Lihong, H., Yong-hong, Z.: The Plasticizing mechanism and effect of aluminium chloride and glycerin on poly(vinyl alcohol) films. Iran. J. Chem. Chem. Eng. **35**(2), 129–135 (2016)

Sakellariou, P., Hassan, A., Rowe, R.C.: Interactions and partitioning of diluents/plasticizers in hydroxypropyl methylcellulose and polyvinyl alcohol homopolymers and blends. Part II: Glycerol. Coll. Polym. Sci. **272**, 48–56 (1994)

Sanyang, M.L., Sapuan, S.M., Jawaid, M., Ishak, M.R., Sahari, J.: Effect of plasticizer type and concentration on tensile, thermal and barrier properties of biodegradable films based on sugar palm (*Arenga pinnata*) Starch. Polymers **7**, 1106–1124 (2015)

Shahbazi, M., Bahari, A., Ghasemi, S.: Studying saturation mobility, threshold voltage, and stability of PMMA-SiO_2-TMSPM nano-hybrid as OFET gate dielectric. Org. Electron. 221, 332–339 (2016)

Shujahadeen Aziz, B., Brza, M.A., Muaffaq Nofal, M., Rebar Abdulwahid, T., Sarkawt Hussen, A., Ahang Hussein, M., Wrya Karim, O.: A comprehensive review on optical properties of polymer electrolytes and composites. Materials **13**, 3675 (2020)

Sugumaran, S., Bellan, C.S., Muthu, D., Raja, S., Bheeman, D., Rajamani, R.: Novel hybrid PVA–InZnO transparent thin films and sandwich capacitor structure by dip coating method: preparation and characterizations. RSC Adv. **5**, 10599–10610 (2015)

Urbach, F.: The long-wavelength edge of photographic sensitivity and of the electronic absorption of solids. Phys. Rev. **92** (5), 1324–1330 (1953)

Yahia, I.S., Mohammed, M.I.: Facile synthesis of graphene oxide/PVA nanocomposites for laser optical limiting: band gap analysis and dielectric constants. Mater. Sci. Mater. Electron. **29**, 8555–8563 (2018)

Yahia, I.S., Mohammed, M.I., Nawar, A.M.: Multifunction applications of TiO_2/poly(vinyl alcohol) nanocomposites for laser attenuation applications. Phys. B Condens. Matter **556**, 48–60 (2019)

Yakuphanoglu, F., Sekerci, M., Balaban, A.: The effect of film thickness on the optical absorption edge and optical constants of the Cr(III) organic thin films. Opt. Mater. **27**, 1369–1372 (2005)

Yassin, A.Y.: Synthesized polymeric nanocomposites with enhanced optical and electrical properties based on gold nanoparticles for optoelectronic applications. Mater. Sci. Mater. Electron. **34**(46), 1–18 (2023)

Yong, L., Xiancai, J., Weiying, Z., Xiao, L.: Effect of aluminium nitrate hydrate on the crystalline, thermal and mechanical properties of poly (vinyl alcohol) Film. Polym. Polym. Compos. **23**(8), 555–562 (2015)

Publisher's Note Springer Nature remains neutral with regard to jurisdictional claims in published maps and institutional affiliations.

Authors and Affiliations

M. I. Mohammed[1,2] · F. El-Sayed[2]

✉ M. I. Mohammed
mrftismail@yahoo.com

F. El-Sayed
asemmohmed2015@gmail.com

[1]   Nanoscience Laboratory for Environmental and Bio-Medical Applications (NLEBA), Green Research Laboratory (GRL), Ain Shams University, Roxy, Cairo 11757, Egypt

[2]   Metallurgical Lab.2, Department of Physics, Faculty of Education, Ain Shams University, Roxy, Cairo 11757, Egypt